Journal of Power Sources 226 (2013) 42–46

Contents lists available at SciVerse ScienceDirect

Journal of Power Sources

journal homepage: www.elsevier.com/locate/jpowsour

Short communication

Resonant photoemission spectroscopy of the cathode material $Li_xMn_{0.5}Fe_{0.5}PO_4$ for lithium-ion battery

Shodai Kurosumi [a], Koji Horiba [a,b,*], Naoka Nagamura [a,b], Satoshi Toyoda [a,b], Hiroshi Kumigashira [c,d], Masaharu Oshima [a,b], Sho Furutsuki [e], Shin-ichi Nishimura [e], Atsuo Yamada [e], Noritaka Mizuno [a]

[a] Department of Applied Chemistry, The University of Tokyo, 7-3-1 Hongo, Bunkyo-ku, Tokyo 113-8656, Japan
[b] Synchrotron Radiation Research Organization, The University of Tokyo, 7-3-1 Hongo, Bunkyo-ku, Tokyo 113-8656, Japan
[c] Photon Factory, Institute of Materials Structure Science, High Energy Accelerator Research Organization, 1-1 Oho, Tsukuba, Ibaraki 305-0801, Japan
[d] Precursory Research for Embryonic Science and Technology, Japan Science and Technology Agency, 4-1-8 Honcho, Kawaguchi, Saitama 332-0012, Japan
[e] Department of Chemical System Engineering, The University of Tokyo, 7-3-1 Hongo, Bunkyo-ku, Tokyo 113-8656, Japan

HIGHLIGHTS

- We reveal the element-specific electronic structure of $Li_xMn_{0.5}Fe_{0.5}PO_4$.
- Changes in the Fe 3*d* states of $Li_xMn_{0.5}Fe_{0.5}PO_4$ are identical with those of Li_xFePO_4.
- Mn 3*d* states of $Li_xMn_{0.5}Fe_{0.5}PO_4$ remain unchanged through the charge reaction.

ARTICLE INFO

Article history:
Received 8 August 2012
Received in revised form
9 October 2012
Accepted 12 October 2012
Available online 30 October 2012

Keywords:
Resonant photoemission spectroscopy
Cathode material
Lithium-ion battery
Olivine-type

ABSTRACT

We have investigated the change in the electronic structure of $Li_xMn_{0.5}Fe_{0.5}PO_4$ through the charge process, especially in the transition metal partial DOS using X-ray absorption and resonant photoemission spectroscopy measurements. The oxidation reaction between Fe^{2+} and Fe^{3+} proceeds while the 0.5 Li ions are extracted from $LiMn_{0.5}Fe_{0.5}PO_4$. Moreover, comparing resonant photoemission spectra of $Li_xMn_{0.5}Fe_{0.5}PO_4$ with those of Li_xFePO_4, we have found that both spectral line-shapes are almost identical, suggesting that the strong localization of the Fe 3*d* states in the $LiMn_{0.5}Fe_{0.5}PO_4$ system. On the other hand, in Mn 2*p*–3*d* X-ray absorption and resonant photoemission spectra, the Mn oxidation reaction from Mn^{2+} to Mn^{3+} partially occurs and Mn 3*d* states of $Li_xMn_{0.5}Fe_{0.5}PO_4$ remain almost unchanged through the charge reaction. Reflecting the difference in the strength of the interaction between the transition metal Fe or Mn ions and the oxygen ions, it is suggested that although the oxidation from Fe^{2+} to Fe^{3+} proceeds largely on Fe ions during the charge reaction from $x = 1.0$ to 0.5, the charge compensation for the electron exchange mainly occurs not only at the Mn ions but also at the poly-anion sites during the charge reaction from $x = 0.5$ to 0.

© 2012 Elsevier B.V. All rights reserved.

1. Introduction

Over the last decade, olivine-type $LiMPO_4$ [M = Fe, Mn, Co, Ni] materials have been attracting much research interest as cathode materials for the lithium-ion battery with low cost, environmental friendliness and high level of safety [1–4]. Moreover, through the M–O–P inductive effect, the presence of poly-anion $(PO_4)^{3-}$ in $LiMPO_4$ makes transition metal atoms strongly ionic and stabilizes anti-bonding states, resulting in generation of high voltage [5–7]. Particularly, the iron-based compound $LiFePO_4$ which shows the redox plateau located at 3.4 V vs. Li/Li^+ has been commercially used in practical applications. Currently, much effort has been made toward the development of new cathode materials exhibiting the positive electrochemical properties of $LiFePO_4$ along with higher energy density. In consideration of the higher energy density, the solid solution $LiMn_yFe_{1-y}PO_4$ is one of the most promising candidates for the alternative cathode materials due to relatively high potential of Mn^{3+}/Mn^{2+} redox couple at 4.1 V vs. Li/Li^+, leading to higher energy density [8–11].

In order to investigate the charge/discharge mechanism of the $LiMn_yFe_{1-y}PO_4$ system, the changes of the Fe and Mn K-edge features through the charge/discharge reactions were previously

* Corresponding author. Department of Applied Chemistry, The University of Tokyo, 7-3-1 Hongo, Bunkyo-ku, Tokyo 113-8656, Japan. Tel.: +81 3 5841 7192; fax: +81 3 5841 8744.
E-mail address: horiba@sr.t.u-tokyo.ac.jp (K. Horiba).

0378-7753/$ – see front matter © 2012 Elsevier B.V. All rights reserved.
http://dx.doi.org/10.1016/j.jpowsour.2012.10.041

analyzed by X-ray absorption near edge structure (XANES) experiments [12–15]. Upon charge reactions, these reports suggested that the Fe^{2+}/Fe^{3+} oxidation reaction proceeds in the 3.4 V region at first and the Mn^{2+}/Mn^{3+} oxidation reaction subsequently proceeds in the 4.1 V region. Moreover, a smaller shift in the Mn K-edge than the Fe K-edge during the Li deintercalation was observed. Although the change in the valence states of the transition metals accompanied with the delithiation have been reported so far, the detailed electronic structure of $LiMn_yFe_{1-y}PO_4$ has not been understood yet. Therefore, in this work, we focus on revealing experimentally the change in the electronic structure of $LiMn_{0.5}Fe_{0.5}PO_4$, especially in the transition metal 3*d* states through the charge process by resonant photoemission spectroscopy (PES).

2. Experimental

Pristine $LiMn_{0.5}Fe_{0.5}PO_4$ powders were synthesized by solid state reactions using Li_2CO_3, $Fe_2C_2O_4{\cdot}2H_2O$, $Mn_2C_2O_4$ and $(NH_4)_2HPO_4$. These starting materials and 10 wt% (as a final product) Ketjen black carbon were poured into a Cr-hardened stainless steel (Cr-ss) container together with a mixture of Cr-ss balls. The precursors were thoroughly mixed and ground by a conventional planetary milling apparatus. The self-assembled $LiMn_{0.5}Fe_{0.5}PO_4$/C composite was synthesized by sintering at 600 °C for 6 h under Ar gas flow. The characterization was performed by X-ray diffraction measurements.

In order to obtain $Li_xMn_{0.5}Fe_{0.5}PO_4$ ($x = 0$, 0.5, 1), an electrochemical delithiation process was carried out. Working electrodes were formulated with the 95 wt% $LiMn_{0.5}Fe_{0.5}PO_4$/C composite and the 5 wt% polytetrafluoroethylene (PTFE) binder. The electrodes were dried at 120 °C in vacuum for a day. The cells were assembled using the above dried working electrode as a positive electrode, Li metal foil as a negative electrode and 1 M $LiPF_6$ dissolved in a mixture of ethylene carbonate/diethyl carbonate (EC/DEC; 3:7 v/v) as an electrolyte in an Ar-filled grove box. The cells were galvanostatically charged and discharged over the potential range from 2.0 V to 4.5 V at the C/10 rate. Fig. 1 shows the charge/discharge curves and cycle performance of the $Li_xMn_{0.5}Fe_{0.5}PO_4$. We confirmed that the large total capacity of 160 mAh g^{-1} were achieved, which is almost identical to the theoretical value, and is highly reversible. After the 3-cycle charge/discharge process to confirm the capacity of the assembled cells, each cell was charged up to 2.0 V, 3.7 V and 4.5 V for lithium compositions *x* of 1, 0.5 and 0, respectively. In the Ar-filled grove box, these $Li_xMn_{0.5}Fe_{0.5}PO_4$ electrodes were separated from the rest of the battery components after cycling and washed with DEC to remove the $LiPF_6$ salt. After being dried, the electrodes were packed into a hermetically sealed bag for transportation.

Spectroscopic experiments were performed at BL-2C of the Photon Factory in High Energy Accelerator Research Organization (KEK-PF). In order to avoid moisture air exposure, we transferred the electrodes to a load lock chamber using a grove bag filled with dry-N_2 gas. To probe the electronic structure of the transition metals such as Fe and Mn 3*d* states in $Li_xMn_{0.5}Fe_{0.5}PO_4$, we have performed Fe and Mn 2*p*–3*d* resonant PES. By resonant PES, we can extract the information on Fe and Mn 3*d* partial density of states (DOS) by gigantic enhancement of photoemission spectra excited with the photons of the energy close to the absorption threshold of Fe and Mn 2*p* core levels, respectively [16–18]. The total energy resolution of PES and X-ray absorption spectroscopy (XAS) measurements was set to 200 meV. The binding energies were calibrated using a C 1*s* core-level peak at 284.4 eV.

Density functional theory (DFT) calculations within an on-site hybrid functional approach were carried out using the full-potential linearized augmented plane-wave method as implemented in the WIEN 2k code. Within this approach, in order to include the effect of electron correlations, we used the PBE0 functional with Hartree–Fock exchange fraction of 0.25.

3. Results and discussion

First of all, we have measured Fe 3*p* and Mn 3*p* core-level spectra of $Li_xMn_{0.5}Fe_{0.5}PO_4$ measured at the photon energy of 600 eV, as shown in Fig. 2. In the Fe 3*p* core level spectra, the energy position of the main peak shifts from 55.6 eV in $LiMn_{0.5}Fe_{0.5}PO_4$ to 56.9 eV in $Li_{0.5}Mn_{0.5}Fe_{0.5}PO_4$ and $Mn_{0.5}Fe_{0.5}PO_4$ due to the valence change from Fe^{2+} to Fe^{3+}. It indicates that the oxidation reaction between Fe^{2+} and Fe^{3+} proceeds while the 0.5 Li ions are extracted from $LiMn_{0.5}Fe_{0.5}PO_4$, which is in good agreement with the electrochemical experiments [2,10–13]. On the other hand, in the Mn 3*p* core level spectra, unexpectedly, the energy position of the main peak almost remains unchanged during the Li deintercalation, which suggests that the oxidation reaction between Mn^{2+} and Mn^{3+} hardly proceeds. In order to investigate the detailed electronic structure, we have performed XAS and resonant PES measurements.

Fig. 3 shows Fe 2*p*–3*d* XAS spectra of $Li_xMn_{0.5}Fe_{0.5}PO_4$. The energy position of the main peak shifts from 708.2 eV in $LiMn_{0.5}Fe_{0.5}PO_4$ to 710.2 eV in $Li_{0.5}Mn_{0.5}Fe_{0.5}PO_4$ and $Mn_{0.5}Fe_{0.5}PO_4$ due to the valence change from Fe^{2+} to Fe^{3+}, which is consistent with the changes of the Fe 3*p* core level spectra. Subsequently, we have measured Fe 2*p*–3*d* resonant PES spectra for each sample with

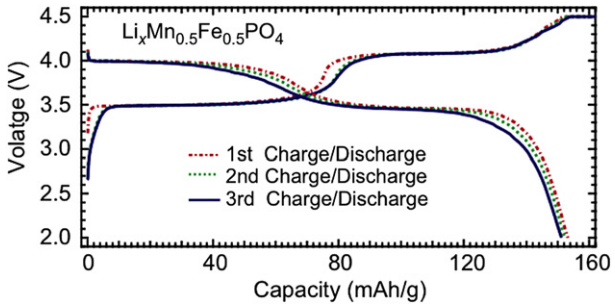

Fig. 1. Galvanostatic charge/discharge curves and cycle performance of the $Li_xMn_{0.5}Fe_{0.5}PO_4$.

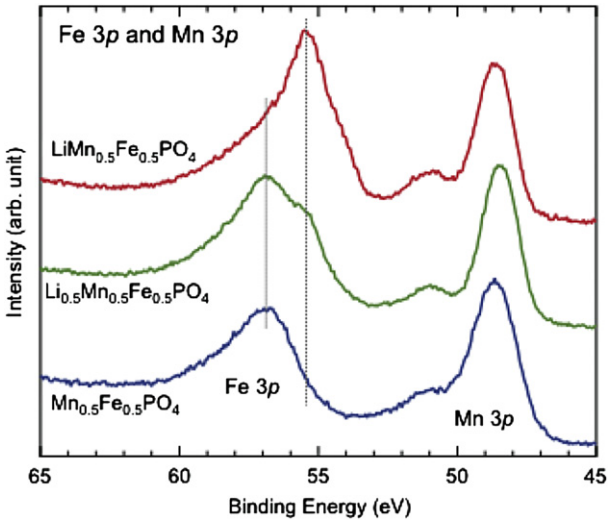

Fig. 2. Fe 3*p* and Mn 3*p* core-level spectra of $Li_xMn_{0.5}Fe_{0.5}PO_4$ measured at the photon energy of 600 eV.

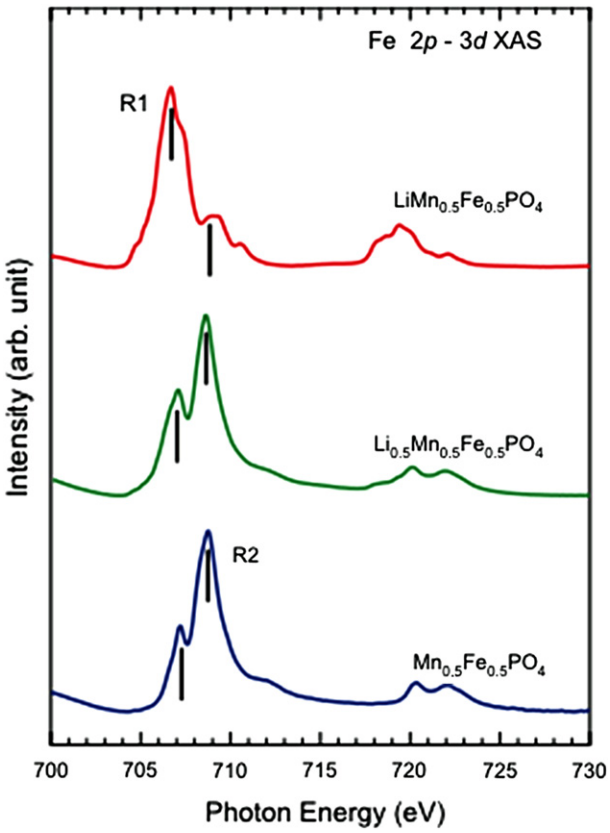

Fig. 3. Fe 2*p*–3*d* XAS spectra of $Li_xMn_{0.5}Fe_{0.5}PO_4$.

excitation energies denoted by the photon energies R1 and R2 corresponding to the absorption edges of Fe^{2+} and Fe^{3+}, respectively. Fig. 4(a) shows the Fe 2*p*–3*d* resonant PES results on $Li_xMn_{0.5}Fe_{0.5}PO_4$. The maximum intensity in the resonant PES spectra was observed at the excitation energy R1 for $LiMn_{0.5}Fe_{0.5}PO_4$, whereas at the excitation energy R2 for $Li_{0.5}Mn_{0.5}Fe_{0.5}PO_4$ and $Mn_{0.5}Fe_{0.5}PO_4$. In comparison between resonant PES spectra for $LiMn_{0.5}Fe_{0.5}PO_4$ and $Li_{0.5}Mn_{0.5}Fe_{0.5}PO_4$, it is found that the spectral line-shape drastically changes in the wide region of valence bands. The first important feature is that the intensity of the peak located at the binding energy of 1.7 eV is enhanced only at the excitation energy R1 corresponding to the photon energy of Fe^{2+} 2*p*–3*d* threshold. This feature indicates that the peak at the binding energy of 1.7 eV can be assigned to the down-spin Fe 3*d* state which exists only in the Fe^{2+} state. The second feature is that the main peak shifts from the binding energy of 5.9 eV in $LiMn_{0.5}Fe_{0.5}PO_4$ to 7.5 eV in $Li_{0.5}Mn_{0.5}Fe_{0.5}PO_4$. The third feature is that Fe 3*d* bands expand into the high binding energy region through the Li deintercalation. These modifications of Fe 3*d* states are explained by the change of the framework structure, where the framework structure of $LiMn_{0.5}Fe_{0.5}PO_4$ shrinks through the Li deintercalation [19]. The same trend is seen with the Fe 3*d* states of Li_xFePO_4, which we previously reported [20]. Therefore, we compared resonant PES spectra of $Li_xMn_{0.5}Fe_{0.5}PO_4$ with that of Li_xFePO_4. Fig. 4(b) shows the resonant PES spectra of $LiFePO_4$ and $LiMn_{0.5}Fe_{0.5}PO_4$ measured at the excitation energy of R1, whereas Fig. 4(c) shows those of $FePO_4$ and $Li_{0.5}Mn_{0.5}Fe_{0.5}PO_4$ measured at the excitation energy of R2. Comparing both resonant PES spectra at each excitation energy, we can find that both spectral-line shapes are almost identical, suggesting that the partial substitution of Fe for Mn does not influence the Fe 3*d* states due to the strong localization of the Fe 3*d* states.

Next, we have measured Mn 2*p*–3*d* XAS spectra of $Li_xMn_{0.5}Fe_{0.5}PO_4$, as shown in Fig. 5(a), in order to investigate the change in Mn 3*d* states during the electrochemical delithiation process. The main peaks in all spectra are located at the photon energy of 639.4 eV, where we can hardly observe the change of spectral line-shape through the Li deintercalation. Judging from the spectral line-shape, Mn^{2+} is the dominant component even after the full delithiation process [21]. In order to illustrate the small change of spectral line-shape, the difference spectrum is obtained by subtracting the spectrum of $Mn_{0.5}Fe_{0.5}PO_4$ from the spectrum of $LiMn_{0.5}Fe_{0.5}PO_4$, as shown in Fig. 5(b). Comparing the difference

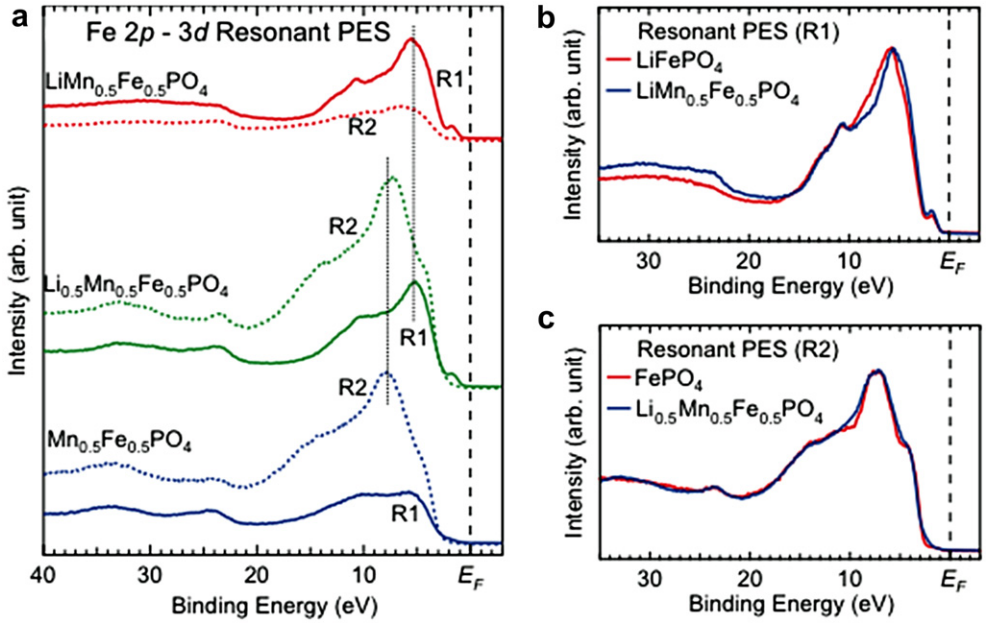

Fig. 4. (a) Fe 2*p*–3*d* resonant PES spectra of $Li_xMn_{0.5}Fe_{0.5}PO_4$ measured at the photon energy of Fe 2*p*–3*d* absorption edge indicated by R1 and R2 in Fig. 3. (b), (c) Fe 2*p*–3*d* resonant PES spectra of $Li_xMn_{0.5}Fe_{0.5}PO_4$ and Li_xFePO_4 measured at R1 and R2, respectively [19].

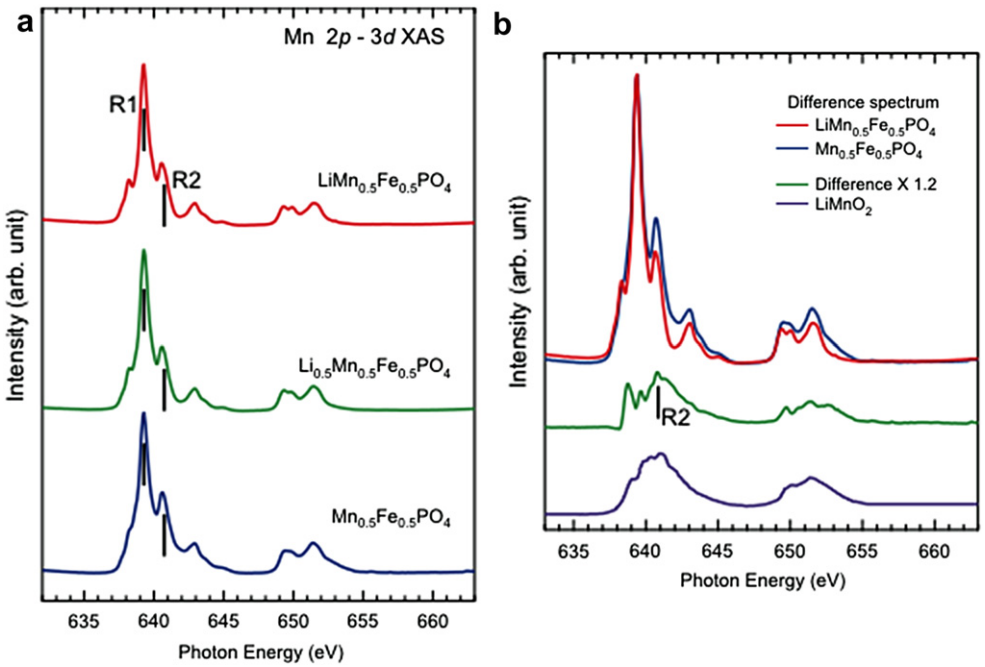

Fig. 5. (a) Mn 2*p*–3*d* XAS spectra of $Li_xMn_{0.5}Fe_{0.5}PO_4$. (b) Difference spectra obtained by subtracting the spectra of $Mn_{0.5}Fe_{0.5}PO_4$ from the spectra of $LiMn_{0.5}Fe_{0.5}PO_4$. The XAS spectrum of $LiMnO_2$ is also shown as the reference data [22].

spectrum with the spectrum of $LiMnO_2$ in which Mn is in the Mn^{3+} oxidation state, we have found a weak Mn^{3+} component [21] in the difference spectrum. The proportion of Mn^{3+} in $Mn_{0.5}Fe_{0.5}PO_4$ corresponding to the intensity ratio of '$Mn_{0.5}Fe_{0.5}PO_4$ − difference' to 'difference' in the spectrum of $Mn_{0.5}Fe_{0.5}PO_4$ is 14%. Although we have also carried out the bulk-sensitive XAS analysis using the fluorescence-yield method with much larger probing depth, the contribution of the Mn^{3+} component is limited to less than 30%. Therefore we think that the low concentration of Mn^{3+} ions in $Mn_{0.5}Fe_{0.5}PO_4$, in other words the difficulty in oxidizing Mn is not due to extrinsic effects such as surface treatments, but due to essential or intrinsic effect in the electrochemical delithiation of $LiMn_{0.5}Fe_{0.5}PO_4$.

Fig. 6 shows the Mn 2*p*–3*d* resonant PES results on $Li_xMn_{0.5}Fe_{0.5}PO_4$ with excitation energies denoted by the photon energies of R1 and R2 in Fig. 5 corresponding to the absorption edges of Mn^{2+} and Mn^{3+}, respectively. The maximum intensity in the resonant PES spectra is observed at the excitation energy of R1 for all samples. Although we observed the slight shift of the main peak, it is found that Mn 3*d* states of $Li_xMn_{0.5}Fe_{0.5}PO_4$ do not change significantly through the Li deintercalation.

From these experimental results, it is found that the electronic structure of Fe in $LiMn_{0.5}Fe_{0.5}PO_4$ changes in the same manner as that in $LiFePO_4$ through the Li deintercalation, whereas the electronic structure of Mn hardly changes. In order to investigate the difference in the charge reaction process between Fe and Mn, we have carried out DFT calculations to analyze the electronic structure of $LiMn_{0.5}Fe_{0.5}PO_4$. Fig. 7 shows the calculated DOS of $LiMn_{0.5}Fe_{0.5}PO_4$. The partial DOS of down-spin Fe 3*d* band, which contributes to the Fe^{3+}/Fe^{2+} charge reaction, is localized at the top of the valence band and hardly overlaps with the O 2*p* partial DOS, indicating the weak interaction between the one down-spin Fe 3*d* state and the O 2*p* state. On the other hand, for the up-spin Mn 3*d* bands which will contribute to the Mn^{3+}/Mn^{2+} charge reaction if the Mn oxidation reaction proceeds, the partial DOS is distributed across the whole valence band and there is a large overlap with the O 2*p* partial DOS. Particularly, it is clearly seen that the line-shape of Mn 3*d* partial DOS at the binding energy of about 2 eV is almost the same as that of O 2*p* partial DOS, suggesting strong hybridization between Mn 3*d* states and O 2*p* states. These characteristic features for the Fe and Mn 3*d* states in $LiMn_{0.5}Fe_{0.5}PO_4$ are similar to those for the Fe 3*d* states in $LiFePO_4$ and the Mn 3*d* states in $LiMnPO_4$ which were previously suggested by the theoretical reports,

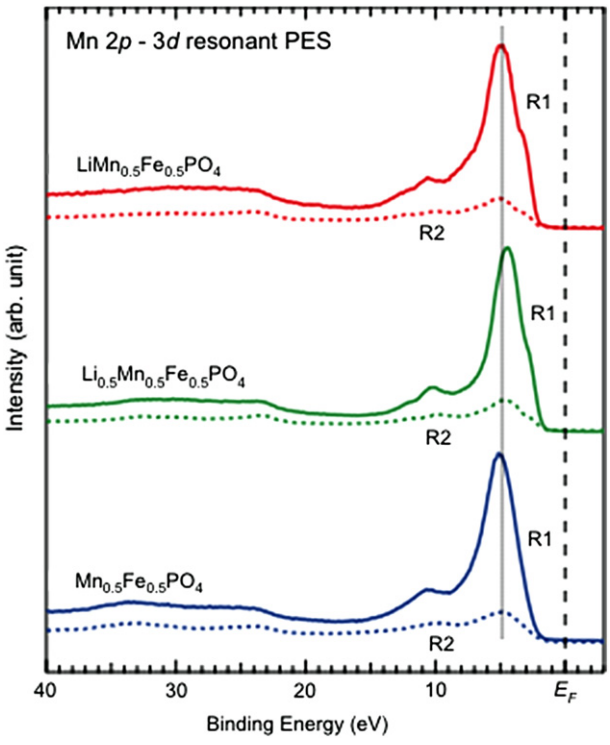

Fig. 6. Mn 2*p*–3*d* resonant PES spectra of $Li_xMn_{0.5}Fe_{0.5}PO_4$ measured at the photon energy of Mn 2*p*–3*d* absorption edge indicated by R1 and R2 in Fig. 5.

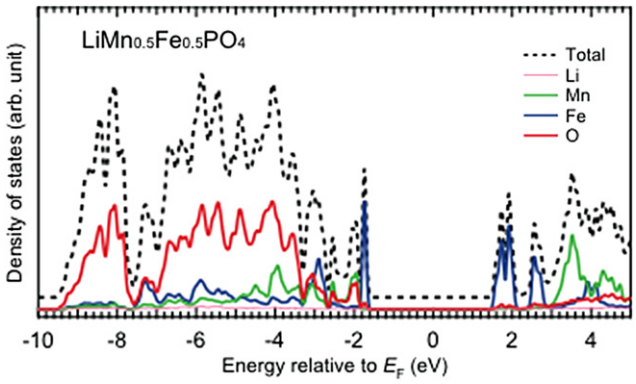

Fig. 7. Total and partial DOSs of $LiMn_{0.5}Fe_{0.5}PO_4$ obtained from DFT calculations. All DOSs are shifted to the high binding energy by 1.7 eV where the energy position of the spin down Fe 3*d* state obtained by DFT calculations are reconciled with the energy position obtained by the experimental results.

respectively [20,23,24]. Reflecting the difference in the strength of the interaction between the transition metal ions and the oxygen ions for Fe and Mn, the oxidation from Fe^{2+} to Fe^{3+} largely proceeds for Fe ions, while the oxidation from Mn^{2+} to Mn^{3+} partially proceeds for Mn ions. In this case, not only the Mn oxidation reaction, but also the charge compensation for the electron exchange at the poly-anion sites [25,26] may occur while the 0.5 Li ions are extracted from $Li_{0.5}Mn_{0.5}Fe_{0.5}PO_4$.

4. Conclusion

We have experimentally revealed the change in the electronic structure of $Li_xMn_{0.5}Fe_{0.5}PO_4$, especially in the transition metal partial DOS through the charge process by XAS and resonant PES measurements. From the Fe 2*p*–3*d* XAS measurements, it is found that the oxidation reaction between Fe^{2+} and Fe^{3+} proceeds while the 0.5 Li ions are extracted from $LiMn_{0.5}Fe_{0.5}PO_4$. Moreover, comparing resonant PES spectra of $Li_xMn_{0.5}Fe_{0.5}PO_4$ with that of Li_xFePO_4, we have found that both spectral line-shapes are almost identical, suggesting that the strong localization of the Fe 3*d* states in the $LiMn_{0.5}Fe_{0.5}PO_4$ system. On the other hand, in Mn 2*p*–3*d* XAS spectra and resonant PES spectra, Mn 3*d* states of $Li_xMn_{0.5}Fe_{0.5}PO_4$ remain almost unchanged through the charge reaction. In order to investigate the difference in the charge reaction process between Fe and Mn ions, we have carried out DFT calculations. Reflecting the difference in the strength of the interaction between the transition metal ions and the oxygen ions for Fe and Mn, the oxidation from Fe^{2+} to Fe^{3+} largely proceeds for Fe ions, while that from Mn^{2+} to Mn^{3+} partially proceeds for Mn ions. It suggests that not only the partial Mn^{3+}/Mn^{2+} charge reaction, but also the charge compensation for the electron exchange at the poly-anion sites occurs while the 0.5 Li ions are extracted from $Li_{0.5}Mn_{0.5}Fe_{0.5}PO_4$.

Acknowledgments

This work is supported by the Japan Society for the Promotion of Science (JSPS) through its “Funding Program for World-Leading Innovative R&D on Science and Technology (FIRST Program).”

References

[1] A. Yamada, S.C. Chung, K. Hinokuma, J. Electrochem. Soc. 148 (2001) A224.
[2] A.K. Padhi, K.S. Nanjundaswamy, J.B. Goodenough, J. Electrochem. Soc. 144 (1997) 1188.
[3] K. Amine, H. Yasuda, M. Yamachi, Electrochem. Solid State Lett. 3 (4) (2000) 178.
[4] J. Wolfenstine, J. Allen, J. Power Sources 142 (2005) 389.
[5] A.K. Padhi, K.S. Nanjyundaswamy, C. Masquelier, S. Okada, J.B. Goodenough, J. Electrochem. Soc. 144 (1997) 1609.
[6] A. Manthiram, J.B. Goodenough, J. Power Sources 26 (1989) 403.
[7] K.S. Nanjyundaswamy, A.K. Padhi, J.B. Goodenough, S. Okada, H. Ohtsuka, H. Arai, J. Yamaki, Solid State Ionics 92 (1996) 1.
[8] A. Yamada, Y. Kudo, K.-Y. Liu, J. Electrochem. Soc. 148 (2001) A1153.
[9] H. Wang, Y. Yang, L.-F. Cui, H.S. Casalomgue, Y. Li, G. Hong, Y. Cui, H. Dai, Angew. Chem. 123 (2011) 7502.
[10] S.-M. Oh, H.-G. Jung, C.S. Yoon, S.-T. Myung, Z. Chen, K. Amine, Y.-K. Sun, J. Power Sources 196 (2011) 6924.
[11] G. Kobayashi, A. Yamada, S. Nishimura, R. Kanno, Y. Kobayashi, S. Seki, Y. Ohno, H. Miyashiro, J. Power Sources 189 (2009) 397.
[12] A. Yamada, Y. Kudo, K.-Y. Liu, J. Electrochem. Soc. 148 (2001) A747.
[13] K.-W. Nam, W.-S. Yoon, K. Zaghib, K.Y. Chung, X.-Q. Yang, Electrochem. Commun. 11 (2009) 2023.
[14] Y.-C. Chen, J.-M. Chen, C.-H. Hsu, J.-F. Lee, J.-W. Yeh, H.C. Shih, Solid State Ionics 180 (2009) 1215.
[15] T. Nedoseykina, M.G. Kim, S.-A. Park, H.-S. Kim, S.-B. Kim, J. Cho, Y. Lee, Electrochim. Acta 55 (2010) 8876.
[16] U. Fano, Phys. Rev. 124 (1961) 1866.
[17] M. Kobayashi, Y. Ooki, M. Takizawa, G.S. Song, A. Fujimori, Y. Takeda, K. Terai, T. Okane, S.I. Fujimori, Y. Saitoh, H. Yamagami, M. Seki, T. Kawai, H. Tabata, Appl. Phys. Chem. *92* (2008) 082502.
[18] H. Kumigashira, D. Kobayashi, R. Hashimoto, A. Chikamatsu, M. Oshima, N. Nakagawa, T. Ohnishi, M. Lippmaa, H. Wadati, A. Fujimori, K. Ono, M. Kawasaki, H. Koinuma, Appl. Phys. Lett. 84 (2004) 5353.
[19] A. Yamada, Y. Takei, H. Koizumi, N. Sonoyama, R. Kanno, Chem. Mater. 18 (2006) 804.
[20] S. Kurosumi, N. Nagamura, S. Toyoda, K. Horiba, H. Kumigashira, M. Oshima, S. Furutsuki, S. Nishimura, A. Yamada, N. Mizuno, J. Phys. Chem. C 115 (2011) 25519.
[21] T. Bunus, Z. Hu, H.H. Hsieh, V.L. Joly, P.A. Joy, M.W. Haverkort, H. Wu, A. Tanaka, H.-J. Lin, C.T. Chen, L.H. Tjeng, Phys. Rev. B 77 (2008) 125124.
[22] F.M.F. de Groot, J. Electron. Spectrosc. Relat. Phenom. 67 (1994) 529.
[23] A. Augustsson, G.V. Zhuang, S.M. Butorin, J.M. Osorio-Guillén, C.L. Dong, R. Ahuja, C.L. Chang, P.N. Ross, J. Nordgren, J.H. Guo, J. Chem. Phys. 123 (2005) 184717.
[24] S.P. Ong, V.L. Chevrier, G. Ceder, Phys. Rev. B *83* (2011) 075112.
[25] A. Yamada, N. Iwane, S. Nishimura, Y. Koyama, I. Tanaka, J. Mater. Chem. 21 (2011) 10690.
[26] S. Laubach, S. Laubach, P.C. Schmidt, D. Ensling, S. Schmid, W. Jaegermann, A. Thißen, K. Nikolowski, H. Ehrenberg, Phys. Chem. Chem. Phys. 11 (2009) 3278.